Robotica (1997) volume 15, pp 563–571. Printed in the United Kingdom © 1997 Cambridge University Press

Experimental Evaluation of Identification Schemes on a Direct Drive Robot*

Fernando Reyes and Rafael Kelly

División de Física Aplicada, CICESE, Apdo. Postal 2615, Adm. 1, Carretera Tijuana-Ensenada Km. 107, Ensenada, B.C. 22800 (Mexico) e-mail: rkelly@cicese.mx. e-mail: freyez@cicese.mx.

(Received in Final Form: December 16, 1996)

SUMMARY

This paper describes the experimental evaluation of three identification schemes to determine the dynamic parameters of a two degrees of freedom direct-drive robot. These schemes involve a recursive estimator while the regression models are formulated in continuous time. The fact that the total energy of robot manipulators can be represented as a linear relation in the inertial parameters, has motivated the suggestion in the literature of several regression models which are linear in a common dynamic parameter vector. Among them, in this paper we consider the schemes based on the filtered dynamic regression model, the supplied energy regression model and a new one proposed in this paper: the filtered power regression model. The underling recursive parameter estimator used in the experimental evaluation is the standard least-squares.

KEYWORDS: Direct drive robot; Identification schemes; Regression model; Filtered power.

1 INTRODUCTION

Identification techniques for robot manipulators are particularly attractive to determine the dynamic parameters of robot manipulators when there exists difficulty to measure them directly. The usefulness of the dynamic parameters arises in implementation of advanced model-based controllers for robot manipulators. The precision, performance, and robustness of these schemes depend on the accuracy of the dynamic model parameters.

A landmark in robot identification has been the recognition that combinations of inertial parameters appear linearly in the dynamic equations of robots manipulators.[1,2] The early identification work exploiting this property of robot dynamics required joint acceleration into the regression model. This approach led to so called the dynamic regression model also known as the differential regression model.[3–5] The first approach relaxing joint acceleration data was proposed by Hsu et al.[6] by introducing the filtered dynamic regression model. Since that time, a number of identification approaches has been suggested in the literaturer;[1,2,6–11] (for an interesting review see Lu et al.[11])

* Work partially supported by CONACYT, Mexico.

The recognition that the total energy of robot manipulators can be described by a linear regression in a combination of the inertial parameters was used to propose the supplied energy regression model[12] also known as the integral model.[3–5] As much as the filtered dynamic model as the supplied energy model are regression models independent of joint acceleration. However, an advantage of the supplied energy model over the filtered dynamic model is that the former yields a scalar prediction error while the latter leads to a vector prediction error.

A modest contribution of this paper is the proposal of a new regression model also based on the principle of energy conservation. We call this model the filtered power model; this is derived from the supplied energy model proposed by Gautier and Khalil.[12] In contrast with the supplied energy model which involves the integral of the power, the new proposed regression model contains a low-pass filter of the power. This filter avoids potential problems owing to the infinite gain of the integrator at zero frequency.

Although there exists a number of references in the literature dealing with robot identification, there have been few works concerning experimental comparison between the use of various regression models. Among the exceptions, Shirkey[5] has performed experimental identification tests with the filtered dynamic model and the supplied energy model on a two degrees of freedom direct drive arm. The conclusion of that work is that the filtered dynamic model is superior to the supplied energy model. Two more exceptions of our special interest that are worth mentioning here are.[3,4] The first one presented a comparison between filtered dynamic and supplied energy model on a direct driven two link robot. It was remarked that the filtered dynamic model has advantages with respect to the supplied energy model. Recently, Kozlowski and Dutkiewicz[4] presented experimental identification using both regression models on a non-direct drive robot. They focus their attention on optimal trajectory design for both models. Their conclusion is also that the filtered dynamic model has advantage in comparison the supplied energy model.

The goal of this paper is to present an experimental comparison of three identification schemes. These schemes belong to the hybrid identification philosophy,[8] i.e. estimation is performed by a recursive estimator while the regression model is formulated in continuous

https://doi.org/10.1017/S0263574797000659 Published online by Cambridge University Press

time. The identification schemes use a common underling recursive estimator: the standard least-squares method, and three different regression models: filtered dynamic model, supplied energy model, and filtered power model. These regression models take into account the friction torques which are assumed to be described by Coulomb and viscous friction models.[13]

The estimated parameters obtained from these identification schemes were compared with the actual parameters of the robot manipulator obtained by direct physical measuring of masses, inertia and center of masses, as well as data provided by the actuator manufacturer. Because sensors accuracy, the measured parameters may not be exact, but they can be considered as the best approximation of the real dynamic parameters. We have also compared open loop responses of the actual robot with simulations using the robot model incorporating the identified parameters.

The organization of this paper is as follows: In Section 2 we recall the robot dynamics. In Section 3 we review the energy model and useful properties. Section 4 presents the identification procedure. The filtered dynamic and supplied energy models are present, then the filtered power model is derived in this section. The experimental implementation is described in Section 5. The experimental results and discussions are presented in Section 6. Finally, we give brief conclusions in Section 7.

2 ROBOT DYNAMICS

The dynamics of a serial n-link rigid robot can be written as:[14]

$$M(\boldsymbol{q})\ddot{\boldsymbol{q}} + C(\boldsymbol{q}, \dot{\boldsymbol{q}})\dot{\boldsymbol{q}} + \boldsymbol{g}(\boldsymbol{q}) + \boldsymbol{f}(\dot{\boldsymbol{q}}) = \boldsymbol{\tau} \tag{1}$$

where $\boldsymbol{q}$ is the $n \times 1$ vector of joint displacements, $\dot{\boldsymbol{q}}$ is the $n \times 1$ vector of joint velocities, $\boldsymbol{\tau}$ is the $n \times 1$ vector of applied torques, $M(\boldsymbol{q})$ is the $n \times n$ symmetric positive definite manipulator inertia matrix, $C(\boldsymbol{q}, \dot{\boldsymbol{q}})$ is the $n \times n$ matrix of centripetal and Coriolis torques, and $\boldsymbol{g}(\boldsymbol{q})$ is the $n \times 1$ vector of gravitational torques obtained as the gradient of the robot potential energy $\mathcal{U}(\boldsymbol{q})$, i.e.

$$\boldsymbol{g}(\boldsymbol{q}) = \frac{\partial \mathcal{U}(\boldsymbol{q})}{\partial \boldsymbol{q}}, \tag{2}$$

and the $n \times 1$ vector $\boldsymbol{f}(\dot{\boldsymbol{q}})$ stands for the friction torques. The friction torque $\boldsymbol{f}(\dot{\boldsymbol{q}})$ is decentralized in the sense that $f_i(\dot{\boldsymbol{q}})$ depends only on $\dot{q}_i$

$$\boldsymbol{f}(\dot{\boldsymbol{q}}) = \begin{bmatrix} f_1(\dot{q}_1) \\ f_2(\dot{q}_2) \\ \vdots \\ f_n(\dot{q}_n) \end{bmatrix}. \tag{3}$$

In this paper we consider the common Coulomb and viscous friction models;[13] that is

$$f_i(\dot{q}_i) = [b_i \dot{q}_i + f_{c_i} \operatorname{sgn}(\dot{q}_i)] \tag{4}$$

where b_i and f_{c_i} represent coefficients of viscous and Coulomb friction for i-th joint respectively.

3 LINEARITY IN THE PARAMETERS OF THE ROBOT TOTAL ENERGY AND DYNAMICS

The purpose of this Section is to recall the property of linearity of the total energy of robot manipulators and that of the robot dynamics, both in terms of the dynamic parameters.

The total energy $\mathcal{E}(\boldsymbol{q}, \dot{\boldsymbol{q}})$ of robot manipulators is given by the sum of the kinetic energy $\mathcal{K}(\boldsymbol{q}, \dot{\boldsymbol{q}})$ plus the potential energy $\mathcal{U}(\boldsymbol{q})$:

$$\mathcal{E}(\boldsymbol{q}, \dot{\boldsymbol{q}}) = \mathcal{K}(\boldsymbol{q}, \dot{\boldsymbol{q}}) + \mathcal{U}(\boldsymbol{q}). \tag{5}$$

The kinetic and potential energy can be written as a linear function of the dynamics parameters:[12]

$$\mathcal{K}(\boldsymbol{q}, \dot{\boldsymbol{q}}) = \phi_{\mathcal{K}}(\boldsymbol{q}, \dot{\boldsymbol{q}})^T \boldsymbol{\theta}_{\mathcal{K}} \tag{6}$$

$$\mathcal{U}(\boldsymbol{q}) = \phi_{\mathcal{U}}(\boldsymbol{q})^T \boldsymbol{\theta}_{\mathcal{U}} \tag{7}$$

where $\phi_{\mathcal{K}}$ and $\phi_{\mathcal{U}}$ are $p_1 \times 1$ and $p_2 \times 1$ vector functions, $\boldsymbol{\theta}_{\mathcal{K}}$ and $\boldsymbol{\theta}_{\mathcal{U}}$ stand for $p_1 \times 1$ and $p_2 \times 1$ vectors which contain the dynamic parameters of the manipulator such as masses and inertia.

Therefore, the total energy (5) can be written as a linear regression in terms of the dynamic parameters:[12]

$$\mathcal{E}(\boldsymbol{q}, \dot{\boldsymbol{q}}) = \phi_{\mathcal{E}}(\boldsymbol{q}, \dot{\boldsymbol{q}})^T \boldsymbol{\theta}_{\mathcal{E}} \tag{8}$$

where $\phi_{\mathcal{E}}(\boldsymbol{q}, \dot{\boldsymbol{q}})^T = [\phi_{\mathcal{K}}(\boldsymbol{q}, \dot{\boldsymbol{q}})^T \quad \phi_{\mathcal{U}}(\boldsymbol{q})^T]$ and

$$\boldsymbol{\theta}_{\mathcal{E}} = [\boldsymbol{\theta}_{\mathcal{K}}^T \quad \boldsymbol{\theta}_{\mathcal{U}}^T]^T. \tag{9}$$

The linear parametrization of the total energy leads to the well known property of linearity in terms of the dynamic parameters for the robot dynamics. For the sake of completeness, let us derive this property.

By using equations (6) and (7), we have that the Lagrangian $\mathcal{L}(\boldsymbol{q}, \dot{\boldsymbol{q}})$ of the robot can be expressed in the form:

$$\mathcal{L}(\boldsymbol{q}, \dot{\boldsymbol{q}}) = \phi_{\mathcal{L}}(\boldsymbol{q}, \dot{\boldsymbol{q}})^T \boldsymbol{\theta}_{\mathcal{E}}$$

where

$$\phi_{\mathcal{L}}(\boldsymbol{q}, \dot{\boldsymbol{q}})^T = [\phi_{\mathcal{K}}(\boldsymbol{q}, \dot{\boldsymbol{q}})^T - \phi_{\mathcal{U}}(\boldsymbol{q})^T]. \tag{10}$$

This yields

$$\frac{\partial \mathcal{L}}{\partial \dot{\boldsymbol{q}}} = \frac{\partial \phi_{\mathcal{L}}(\boldsymbol{q}, \dot{\boldsymbol{q}})}{\partial \dot{\boldsymbol{q}}} \boldsymbol{\theta}_{\mathcal{E}}, \quad \frac{d}{dt}\left[\frac{\partial \mathcal{L}}{\partial \dot{\boldsymbol{q}}}\right] = \left[\frac{d}{dt}\frac{\partial \phi_{\mathcal{L}}(\boldsymbol{q}, \dot{\boldsymbol{q}})}{\partial \dot{\boldsymbol{q}}}\right]\boldsymbol{\theta}_{\mathcal{E}},$$

$$\frac{\partial \mathcal{L}}{\partial \boldsymbol{q}} = \frac{\partial \phi_{\mathcal{L}}(\boldsymbol{q}, \dot{\boldsymbol{q}})}{\partial \boldsymbol{q}} \boldsymbol{\theta}_{\mathcal{E}}.$$

By considering as the generalized nonconservative forces those owing to the applied torques/forces $\boldsymbol{\tau}$ and the friction forces $\boldsymbol{f}(\dot{\boldsymbol{q}})$, from the Lagrange's equation of motion we obtain

$$\left[\frac{d}{dt}\left[\frac{\partial \phi_{\mathcal{L}}(\boldsymbol{q}, \dot{\boldsymbol{q}})}{\partial \dot{\boldsymbol{q}}}\right] - \frac{\partial \phi_{\mathcal{L}}(\boldsymbol{q}, \dot{\boldsymbol{q}})}{\partial \boldsymbol{q}}\right]\boldsymbol{\theta}_{\mathcal{E}} = \boldsymbol{\tau} - \boldsymbol{f}(\dot{\boldsymbol{q}}). \tag{11}$$

Due to the fact that the friction force present in the robot is assumed be Coulomb and viscous friction, then it

https://doi.org/10.1017/S0263574797000659 Published online by Cambridge University Press

is linear with respect to the coefficients of Coulomb and viscous friction, this is:

$$\boldsymbol{f}(\dot{\boldsymbol{q}}) = \phi_{\mathscr{F}}(\dot{\boldsymbol{q}})\boldsymbol{\theta}_{\mathscr{F}} \tag{12}$$

where $\phi_{\mathscr{F}}$ is an $n \times 2n$ matrix function and $\boldsymbol{\theta}_{\mathscr{F}}$ stands $2n \times 1$ vector, which contains the Coulomb and viscous friction coefficients. Therefore the equation (11) can be written as:

$$\underbrace{\left[\left[\frac{d}{dt}\left[\frac{\partial \phi_{\mathscr{L}}(\boldsymbol{q}, \dot{\boldsymbol{q}})}{\partial \dot{\boldsymbol{q}}}\right] - \frac{\partial \phi_{\mathscr{L}}(\boldsymbol{q}, \dot{\boldsymbol{q}})}{\partial \boldsymbol{q}}\right] \quad \phi_{\mathscr{F}}(\dot{\boldsymbol{q}})\right]}_{Y(\boldsymbol{q}, \dot{\boldsymbol{q}}, \ddot{\boldsymbol{q}})}\boldsymbol{\theta} = \boldsymbol{\tau} \tag{13}$$

where

$$\boldsymbol{\theta} = [\boldsymbol{\theta}_{\mathscr{E}}^T \quad \boldsymbol{\theta}_{\mathscr{F}}^T]^T \tag{14}$$

denotes the vector of the dynamic and friction parameters.

Finally, from the robot dynamics (1) and (13) we get the well established fundamental property of the robot dynamics of being linear in the dynamic parameters,[1,2] i.e.

$$M(\boldsymbol{q})\ddot{\boldsymbol{q}} + C(\boldsymbol{q}, \dot{\boldsymbol{q}})\dot{\boldsymbol{q}} + \boldsymbol{g}(\boldsymbol{q}) + \boldsymbol{f}(\dot{\boldsymbol{q}}) = Y(\boldsymbol{q}, \dot{\boldsymbol{q}}, \ddot{\boldsymbol{q}})\boldsymbol{\theta} = \boldsymbol{\tau} \tag{15}$$

where $Y(\boldsymbol{q}, \dot{\boldsymbol{q}}, \ddot{\boldsymbol{q}})$ is an $n \times p$ matrix of known functions, $\boldsymbol{\theta}$ is $p \times 1$ vector containing the robot and friction parameters, and $p = p_1 + p_2 + 2n$.

4 PARAMETER IDENTIFICATION

In this Section we describe three identification schemes. Each scheme arises from a common recursive estimator, in this case the least squares method, and the corresponding regression model. Before we introduce the regression models, we outline the standard least-squares algorithm.

4.1 Least-squares algorithm

The least-squares method is a basic technique for parameter estimation. The method is particularly simple if the model has the property of being linear in the parameters. Let us consider the following regression model

$$\boldsymbol{y}(k) = \Psi(k)^T\boldsymbol{\theta} \tag{16}$$

where $\boldsymbol{y}(k)$ represents an $n \times 1$ output vector, $\Psi(k)$ stands for the $p \times n$ regressor matrix of known functions, and $\boldsymbol{\theta}$ is the $p \times 1$ vector of unknown parameters. The model is indexed by the variable k, which denotes the sampling time. It will be assumed that the index set is a discrete set.

The unknown parameters $\boldsymbol{\theta}$ can be estimated by minimizing the following cost function:[15,16]

$$J_k(\boldsymbol{\theta}) = \frac{1}{2}\sum_{i=1}^{k}[\boldsymbol{y}(i) - \Psi(i)^T\boldsymbol{\theta}]^T[\boldsymbol{y}(i) - \Psi(i)^T\boldsymbol{\theta}] + \frac{1}{2}[\boldsymbol{\theta} - \hat{\boldsymbol{\theta}}(0)]^T P(0)^{-1}[\boldsymbol{\theta} - \hat{\boldsymbol{\theta}}(0)] \tag{17}$$

where $P(0) = P(0)^T > 0$ and $\hat{\boldsymbol{\theta}}(0)$ denotes the initial estimate.

The value estimated of vector $\boldsymbol{\theta}$ based on the observations of the vector $\boldsymbol{y}(k)$ and of the regressor $\Psi(k)$ is obtained by minimizing cost function (17), which we denote as $\hat{\boldsymbol{\theta}}(k)$ satisfying the following equation:

$$\hat{\boldsymbol{\theta}}(k) = P(k)\left[P(0)^{-1}\hat{\boldsymbol{\theta}}(0) + \sum_{i=1}^{k}\Psi(i)\boldsymbol{y}(i)\right] \tag{18}$$

$$P(k) = \left[P(0)^{-1} + \sum_{i=1}^{k}\Psi(i)\Psi(i)^T\right]^{-1} \tag{19}$$

where $P(k)$ is $n \times n$ matrix called covariance matrix.

The recursive version of the least-squares method is given by the well known equations:[15,16]

$$\hat{\boldsymbol{\theta}}(k) = \hat{\boldsymbol{\theta}}(k-1) + P(k-1)\Psi(k) \times [I + \Psi(k)^T P(k-1)\Psi(k)]^{-1}e(k) \tag{20}$$

$$P(k) = P(k-1) - P(k-1)\Psi(k) \times [I + \Psi(k)^T P(k-1)\Psi(k)]^{-1}\Psi(k)^T P(k-1) \tag{21}$$

where the prediction error $e(k)$ is defined as:

$$e(k) = \boldsymbol{y}(k) - \Psi(k)^T\hat{\boldsymbol{\theta}}(k-1). \tag{22}$$

4.2 Filtered dynamic regression model

The robot dynamic model (15), which finally serves for robot control, relates the torques applied on the joints to the regressor matrix $Y(\boldsymbol{q}, \dot{\boldsymbol{q}}, \ddot{\boldsymbol{q}})$ and the vector of unknown dynamic parameters $\boldsymbol{\theta}$. This leads to the dynamic regression model also so-called the differential regression model:[3–5]

$$\boldsymbol{\tau} = Y(\boldsymbol{q}, \dot{\boldsymbol{q}}, \ddot{\boldsymbol{q}})\boldsymbol{\theta}. \tag{23}$$

Notice that to compute the elements of $Y(\boldsymbol{q}, \dot{\boldsymbol{q}}, \ddot{\boldsymbol{q}})$, one needs the measurement of joint acceleration $\ddot{\boldsymbol{q}}$. To overcome this shortcoming the filtered dynamic regression model has been proposed in the literature.[6,9–11]

The key idea is to filter both sides of the robot dynamics (23) by a stable strictly proper filter. Without lost of generality, the simple first order filter has been considered in most previous works.[6,9–11]. Let us denote this filter by its transfer function $f(s) = \dfrac{\lambda}{s + \lambda}$, where $\lambda > 0$ and s stands for the differential operator. Therefore, the filtered dynamic regression model can be written as

$$\boldsymbol{\tau}_f = Y_f(\boldsymbol{q}, \dot{\boldsymbol{q}})\boldsymbol{\theta}$$

where

$$\boldsymbol{\tau}_f = f(s)\boldsymbol{\tau}$$
$$Y_f(\boldsymbol{q}, \dot{\boldsymbol{q}}) = f(s)Y(\boldsymbol{q}, \dot{\boldsymbol{q}}, \ddot{\boldsymbol{q}}).$$

Thanks to the introduction of the filters, the requirement of joint acceleration $\ddot{\boldsymbol{q}}$ into the regressor $Y_f(\boldsymbol{q}, \dot{\boldsymbol{q}})$ has been obviated.

With above notation, and with reference to the recursive least-squares method, the prediction error corresponding to the filtered dynamic regression model takes the form

$$e(k) = \underbrace{\boldsymbol{\tau}_f(k)}_{\boldsymbol{y}(k)} - \underbrace{Y_f(\boldsymbol{q}, \dot{\boldsymbol{q}})(k)}_{\Psi(k)^T}\hat{\boldsymbol{\theta}}(k-1). \tag{24}$$

4.3 Supplied energy regression model

In this subsection we recall the derivation of the supplied energy regression model introduced by Gautier and Khalil.[12]

https://doi.org/10.1017/S0263574797000659 Published online by Cambridge University Press

The principle of conservation of energy states that the work of the forces applied to a system and which are not derived of potential is equal to the change of the total energy of the system, i.e.,

$$\underbrace{\int_0^t \boldsymbol{\tau}(\sigma)^T \dot{\boldsymbol{q}}(\sigma) d\sigma}_{\text{Energy supplied at the instant } t} = \underbrace{\mathscr{E}(\boldsymbol{q}(t), \dot{\boldsymbol{q}}(t)) - \mathscr{E}(\boldsymbol{q}(0), \dot{\boldsymbol{q}}(0))}_{\text{Energy stored at the instant } t} + \underbrace{\int_0^t \dot{\boldsymbol{q}}(\sigma)^T \boldsymbol{f}(\dot{\boldsymbol{q}}(\sigma)) d\sigma}_{\text{Energy dissipated at the instant } t} \quad (25)$$

Without loss of generality, we suppose that total energy at the instant zero is null, that is

$$\mathscr{E}(\boldsymbol{q}(0), \dot{\boldsymbol{q}}(0)) = 0. \quad (26)$$

From principle of conservation of energy and by using the equations (8) and (12), then we obtain the supplied energy regression model:[12]

$$\int_0^t \boldsymbol{\tau}(\sigma)^T \dot{\boldsymbol{q}}(\sigma) d\sigma = \left[\phi_{\mathscr{E}}(\boldsymbol{q}(t), \dot{\boldsymbol{q}}(t))^T \int_0^t \dot{\boldsymbol{q}}(\sigma)^T \phi_{\mathscr{F}}(\dot{\boldsymbol{q}}(\sigma)) d\sigma \right] \boldsymbol{\theta}, \quad (27)$$

which is linear in the dynamic and friction parameters and the regressor depends on $\boldsymbol{q}$ and $\dot{\boldsymbol{q}}$. It does not require the measurement of joint acceleration $\ddot{\boldsymbol{q}}$.

Therefore, the prediction error of the supplied energy regression model for its use in the recursive least-squares algorithm is defined as:

$$e(k) = \underbrace{\int_0^{kh} \boldsymbol{\tau}(\sigma)^T \dot{\boldsymbol{q}}(\sigma) d\sigma}_{y(k)} - \underbrace{\left[\phi_{\mathscr{E}}(\boldsymbol{q}, \dot{\boldsymbol{q}})^T(k) \int_0^{kh} \dot{\boldsymbol{q}}(\sigma)^T \phi_{\mathscr{F}}(\dot{\boldsymbol{q}}(\sigma)) d\sigma \right]}_{\Psi(k)^T} \hat{\boldsymbol{\theta}}(k-1) \quad (28)$$

where h denotes the sampling period.

It is worth noting that this prediction error is a scalar function while in the filtered dynamic model it was a vector function.

4.4 Filtered power regression model

Now, we are in position to formulate a new regression model. The idea is to filter both sides of the supplied energy model (27) via a stable strictly proper filter. Without lost of generality, let us consider again the first order filter whose transfer function is given by $f(s) = \lambda/(s+\lambda)$ where $\lambda > 0$.

By applying the filter to both sides of (27) we obtain the following model, which is called here the filtered power regression model:

$$\frac{\lambda}{s+\lambda} \boldsymbol{\tau}^T(t) \dot{\boldsymbol{q}}(t) = \left[\frac{\lambda s}{s+\lambda} \phi_{\mathscr{E}}(\boldsymbol{q}(t), \dot{\boldsymbol{q}}(t))^T, \frac{\lambda}{s+\lambda} \dot{\boldsymbol{q}}^T \phi_{\mathscr{F}}(\dot{\boldsymbol{q}}) \right] \boldsymbol{\theta}. \quad (29)$$

which is linear in the dynamic and friction parameters and it depends on $\boldsymbol{q}$ and $\dot{\boldsymbol{q}}$ but not on the joint acceleration $\ddot{\boldsymbol{q}}$. The left hand side of (29) is the regression model output; this is the filtering of the power $\boldsymbol{\tau}^T \dot{\boldsymbol{q}}$.

Let the scalar prediction error of the filtered power regression model be defined as:

$$e(k) \underbrace{= \frac{\lambda}{s+\lambda} (\boldsymbol{\tau}^T \dot{\boldsymbol{q}})(k)}_{y(k)} - \underbrace{\left[\frac{\lambda s}{s+\lambda} \phi_{\mathscr{E}}(\boldsymbol{q}, \dot{\boldsymbol{q}})^T(k), \frac{\lambda}{s+\lambda} \dot{\boldsymbol{q}}^T \phi_{\mathscr{F}}(\dot{\boldsymbol{q}})(k) \right]}_{\Psi(k)^T} \hat{\boldsymbol{\theta}}(k-1). \quad (30)$$

5 EXPERIMENTAL IMPLEMENTATION

We have designed and built at CICESE Research Center a direct drive vertical robot manipulator with two degrees of freedom moving in the vertical plane (see Figure 1). It consists of two links made of 6061 aluminum both actuated by brushless direct drive servo actuator to drive the joints without gear reduction. Advantages of this type of direct-drive actuator includes freedom from backslash and significantly lower joint friction compared to actuators with gear drives.[17] The motors used in the robot manipulator are the DM1200-A and DM1015-B models from Parker Compumotor for the shoulder and elbow joints respectively. The servos are operated in torque mode, so the motors act as torque source and they accept an analog voltage as a reference of torque signal. In this configuration the motor DM1200-A is capable to deliver 200 Nm torque output and the motor DM1015-B only 15 Nm.

Position information is obtained from incremental encoders located on the motors which have a resolution of 1024000 p/rev for the first motor and 655360 p/rev for the second one. The accuracy for both motors is 30 arc-seconds.

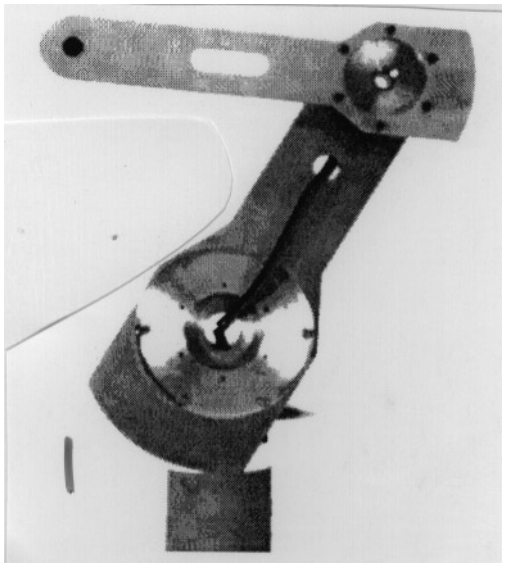


Fig. 1. Experimental robot manipulator.

https://doi.org/10.1017/S0263574797000659 Published online by Cambridge University Press

A motion control board based on a TMS320C31 32-bit floating point microprocessor from Texas Instruments, is used to execute the control algorithm. This board is mounted in a PC 486DX2 host computer which contains a software environment that has been developed to give an user-friendly interface and easy control over experiment set-up, execution, data recording, graphics, display and home return.[18]

In the particular case of our experimental arm the entries of the robot dynamics are given

$$M(\boldsymbol{q}) = \begin{bmatrix} \theta_1 + 2\theta_2 \cos(q_2) & \theta_3 + \theta_2 \cos(q_2) \\ \theta_3 + \theta_2 \cos(q_2) & \theta_3 \end{bmatrix},$$

$$C(\boldsymbol{q}, \dot{\boldsymbol{q}}) = \begin{bmatrix} -2\theta_2 \sin(q_2)\dot{q}_2 & -\theta_2 \sin(q_2)\dot{q}_2 \\ \theta_2 \sin(q_2)\dot{q}_1 & 0 \end{bmatrix},$$

$$\boldsymbol{g}(\boldsymbol{q}) = \begin{bmatrix} \theta_4 \sin(q_1) + \theta_5 \sin(q_1 + q_2) \\ \theta_5 \sin(q_1 + q_2) \end{bmatrix},$$

$$\boldsymbol{f}(\dot{\boldsymbol{q}}) = \begin{bmatrix} \theta_6 \dot{q}_1 + \theta_8 \operatorname{sgn}(\dot{q}_1) \\ \theta_7 \dot{q}_2 + \theta_9 \operatorname{sgn}(\dot{q}_2) \end{bmatrix}$$

where the dynamic and friction parameters are given by

$$\theta_1 = m_1 l_{c1}^2 + m_2 l_1^2 + m_2 l_{c2}^2 + I_1 + I_2$$
$$\theta_2 = l_1 m_2 l_{c2}$$
$$\theta_3 = m_2 l_{c2}^2 + I_2$$
$$\theta_4 = g(l_{c1} m_1 + m_2 l_1)$$
$$\theta_5 = g m_2 l_{c2}$$
$$\theta_6 = b_1$$
$$\theta_7 = b_2$$
$$\theta_8 = f_{c1}$$
$$\theta_9 = f_{c2}.$$

The parameters θ_i, $i = 1 \cdots 9$ can be interpreted as a combinations of some physical properties of the links which are time-invariant. The individual robot parameters are defined in Table I.

With reference to the parametrization of the kinetic and potential energies, the vector of dynamic parameters $\boldsymbol{\theta}$ are related by

$$\boldsymbol{\theta}_{\mathscr{E}} = [\theta_1 \quad \theta_2 \quad \theta_3 \quad \theta_4 \quad \theta_5]^T,$$
$$\boldsymbol{\theta}_{\mathscr{F}} = [\theta_6 \quad \theta_7 \quad \theta_8 \quad \theta_9]^T,$$
$$\boldsymbol{\theta} = [\boldsymbol{\theta}_{\mathscr{E}}^T \quad \boldsymbol{\theta}_{\mathscr{F}}^T]^T.$$

In a first stage, the values of robot parameters shown in Table I were obtained by direct physically measuring. We disassembly the robot manipulator in order to measure its parameters. The mass of each component was determined with a beam balance, while rotor masses were provided from manufacturer;[19] the center gravity of each link was located orthogonal to rotation axis by balancing each link. The moments of inertia of each joint motors were provided from manufacturer[19] and moments of inertia of link were measured by timing oscillations about an axis perpendicular to the plane in which the robot operates and using the equation of motion for a physical pendulum. Moments of inertia for the composite links (link, servo rotor, bolts, etc.) were determined by summing the inertia of the components about the servo axis and applying the parallel axis theorem. The friction coefficients were measured by using a proportional controller of velocity.

An important constituent of identification schemes that requires a more careful and systematic investigation is the choice of a class of input trajectories for exciting the robot. The selection of trajectories must be such that it allows complete identification of the system. This class of trajectories is known as a *persistently exciting trajectory*.[16] Furthermore, the trajectory must foresee the actuators from torque saturating and velocity overflow. Choosing a persistently exciting trajectory is sufficiently complex and has not been addressed in this work.[20]

During the preliminary experiments, we have tested several torque trajectories being linear of sinusoidal functions that contain superposition of four different frequencies to excite the system. The best result of parameter identification were obtained by using the following trajectories

$$\tau_1 = (1 - e^{-0.8t})29.0 + 68 \sin(16t + 0.1) + 9 \sin(20t + 0.15) \ \text{[Nm]}, \tag{31}$$

$$\tau_2 = (1 - e^{-1.8t})1.2 + 8 \sin(26t + 0.08) + 2 \sin(12t + 0.34) \ \text{[Nm]}. \tag{32}$$

Table I. Parameter values.

Parameter	Notation	Value	Unit
Length link 1	l_1	0.45	m
Mass link 1	m_1	23.902	Kg
Mass link 2	m_2	3.880	Kg
Link (1) center of mass	l_{c1}	0.091	m
Link (2) center of mass	l_{c2}	0.048	m
Inertia link 1	I_1	1.266	Kg m^2
Inertia link 2	I_2	0.093	Kg m^2
Viscous coefficient 1	b_1	2.288	Nm-sec
Viscous coefflcient 2	b_2	0.175	Nm-sec
Coulomb coefficient 1	f_{c_1}	7.17 and if $\dot{q}_1 > 0$ and 8.049 if $\dot{q}_1 < 0$	Nm
Coulomb coefficient 2	f_{c_2}	1.734	Nm
Gravity acceleration	g	9.81	m/sec^2

https://doi.org/10.1017/S0263574797000659 Published online by Cambridge University Press

All identification schemes as well as the torque input trajectory were written in *C* language; the sampling period h used in all the experiments was $h = 2.5$ msec. The joint velocity was computed through a standard backwards difference algorithm applied to the position measurement. In the experiments the arm started at rest from its vertical position downward. This produces the following initial conditions: $q_1(0) = q_2(0) = 0$, and $\dot{q}_1(0) = \dot{q}_2(0) = 0$.

In order to validate the values of the robot parameters obtained by direct measurement given in Table I, we have performed simulations and experiments on the actual robot arm using the torque inputs (31)–(32). Figure 2 shows the joint positions obtained in both cases. Notice that the results from simulation, which uses the values of the robot parameters given in Table I, have a good matching with the experimental ones. This allows the conclusion that parameters given in Table I produces a model of the real robot reflecting with good precision its dynamic behavior.

5.1 Filtered dynamic model

The prediction error for the filtered regression model is described by (24). For our arm, the regressor is given by

$$Y_f(\boldsymbol{q}, \dot{\boldsymbol{q}}) = \begin{bmatrix} \frac{\lambda s}{s+\lambda}\dot{q}_1 & \frac{\lambda s}{s+\lambda}\cos(q_2)(2\dot{q}_1 + \dot{q}_2) & \\ 0 & \begin{bmatrix} \frac{\lambda s}{s+\lambda}\cos(q_2)\dot{q}_1 + \\ \frac{\lambda}{s+\lambda}\sin(q_2)(\dot{q}_1 + \dot{q}_2)\dot{q}_1 \end{bmatrix} & \\ \frac{\lambda s}{s+\lambda}\dot{q}_2 & \frac{\lambda}{s+\lambda}\sin(q_1) & \frac{\lambda}{s+\lambda}\sin(q_1+q_2) \\ \frac{\lambda s}{s+\lambda}(\dot{q}_1+\dot{q}_2) & 0 & \frac{\lambda}{s+\lambda}\sin(q_1+q_2) \\ \frac{\lambda}{s+\lambda}\dot{q}_1 & 0 & \frac{\lambda}{s+\lambda}\operatorname{sgn}(\dot{q}_1) \quad 0 \\ 0 & \frac{\lambda}{s+\lambda}\dot{q}_2 & 0 \quad \frac{\lambda}{s+\lambda}\operatorname{sgn}(\dot{q}_2) \end{bmatrix}.$$

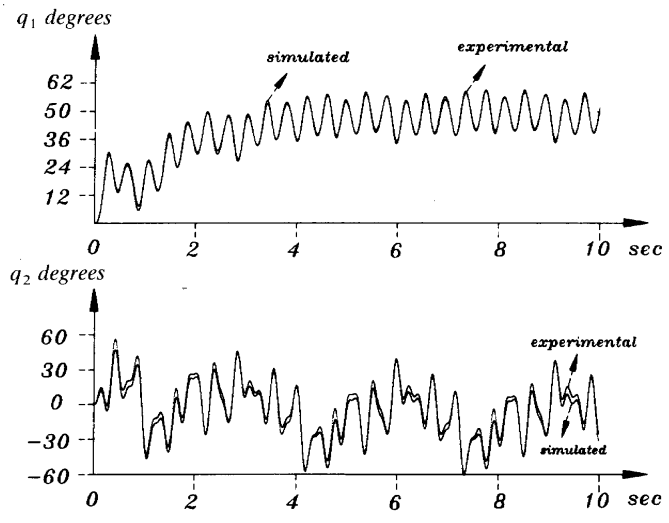


Fig. 2. Simulated and experimental open-loop responses.

Since joint torques, positions, and velocities are hold constant between sampling instant, the filters $f(s) = \frac{\lambda}{s+\lambda}$ and $f(s) = \frac{\lambda s}{s+\lambda}$ can be implemented in form discrete as $f(z^{-1}) = \frac{(1-e^{-h\lambda})z^{-1}}{1-e^{-h\lambda}z^{-1}}$ and $f(z^{-1}) = \frac{(1-z^{-1})\lambda}{1-e^{-h\lambda}z^{-1}}$ respectively.

5.2 Supplied energy model

The prediction error of the supplied energy regression model is given by equation (28). In its adaptation to our direct-drive robot, the regressor takes the form

$$\left[\phi_{\mathscr{E}}(\boldsymbol{q}, \dot{\boldsymbol{q}})^T \int_0^{kh} \dot{\boldsymbol{q}}(\sigma)^T \phi_{\mathscr{F}}(\dot{q}(\sigma))d\sigma\right]$$
$$= \left[\tfrac{1}{2}\dot{q}_1^2 \quad \cos(q_2)\dot{q}_1(\dot{q}_1+\dot{q}_2) \quad \dot{q}_2(\dot{q}_1+\tfrac{1}{2}\dot{q}_2) \quad 1-\cos(q_1)\right.$$
$$\left. 1-\cos(q_1+q_2) \quad \int_0^{kh}\dot{q}_1^2\,d\sigma \quad \int_0^{kh}\dot{q}_2^2 d\sigma \quad \int_0^{kh}|\dot{q}_1|\,d\sigma \quad \int_0^{kh}|\dot{q}_2|\,d\sigma\right].$$

The integrals of regressor matrix have been implemented with a standard trapezoid-type integration rule.

5.3 Filtered power model

The prediction error of the filtered power regression model was defined in (30). The regressor becomes in this case

$$\left[\frac{\lambda s}{s+\lambda}\phi_{\mathscr{E}}(\boldsymbol{q}, \dot{\boldsymbol{q}})^T \quad \frac{\lambda}{s+\lambda}\dot{\boldsymbol{q}}^T\phi_{\mathscr{F}}(\dot{\boldsymbol{q}})(k)\right]$$
$$= \left[\frac{\lambda s}{s+\lambda}\frac{\dot{q}_1^2}{2} \quad \frac{\lambda s}{s+\lambda}\cos(q_2)\dot{q}_1(\dot{q}_1+\dot{q}_2) \quad \frac{\lambda s}{s+\lambda}\dot{q}_2\left(\dot{q}_1+\frac{\dot{q}_2}{2}\right)\right.$$
$$\frac{\lambda s}{s+\lambda}[1-\cos(q_1)] \quad \frac{\lambda s}{s+\lambda}[1-\cos(q_1+q_2)]$$
$$\left.\frac{\lambda}{s+\lambda}\dot{q}_1^2 \quad \frac{\lambda}{s+\lambda}\dot{q}_2^2 \quad \frac{\lambda}{s+\lambda}|\dot{q}_1| \quad \frac{\lambda}{s+\lambda}|\dot{q}_2|\right].$$

The filters $f(s) = \lambda/(s+\lambda)$ invoked in the regressor have been implemented in a recursive manner in the same way that those of the filtered dynamic model.

6 EXPERIMENTAL RESULTS

In this Section we describe the experimental results obtained from the three identification schemes. For the three cases, the recursive least-squares algorithm (20)–(21) was employed with the following initial conditions: the covariance matrix $P(0) =$ diag (1000, 1000, 1000, 1000, 1000, 1000, 1000, 1000, 1000) and the initial vector of estimated parameters $\hat{\boldsymbol{\theta}}(0) = 0$. The bandwidth λ of the filters used in the regressors must be chosen such that it reject the high-frequency components resulting from noise while allowing the low-frequency components generated by the torque input command. The highest frequency in the command trajectory was of $\omega = 26$ rad/s. Therefore we have chosen $\lambda = 50$ Hz.

6.1 Filtered dynamic model

Figure 3 shows the experimental profiles for the estimation vector $\hat{\boldsymbol{\theta}}(k)$ obtained with the filtered dynamic regression model. We observe the convergence in all parameter estimates. Their values at $t = 10$ sec. are summarized in Table II. The accuracy in the estimated

https://doi.org/10.1017/S0263574797000659 Published online by Cambridge University Press

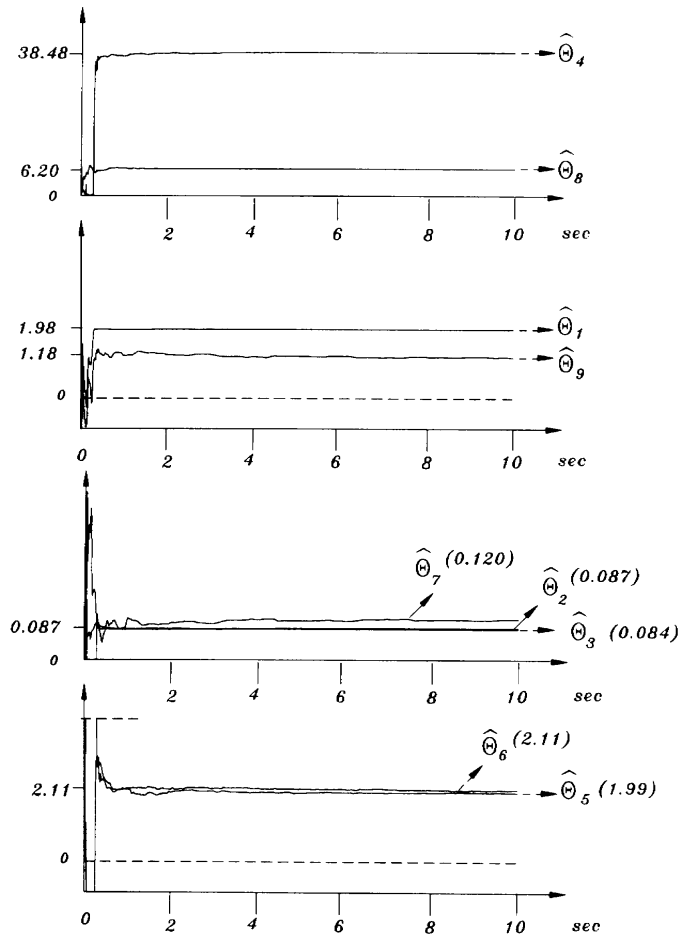


Fig. 3. Estimated vector $\hat{\boldsymbol{\theta}}$ of the filtered dynamic model.

dynamic parameters (excluding friction parameters) is found between 82% and 97% with respect to the parameters obtained by direct physically measuring. However the estimated friction coefficients have a larger deviation.

Despite the deviation of the estimated values with respect to those computed from direct measurement, the open-loop responses depicted in Figure 4 illustrate that

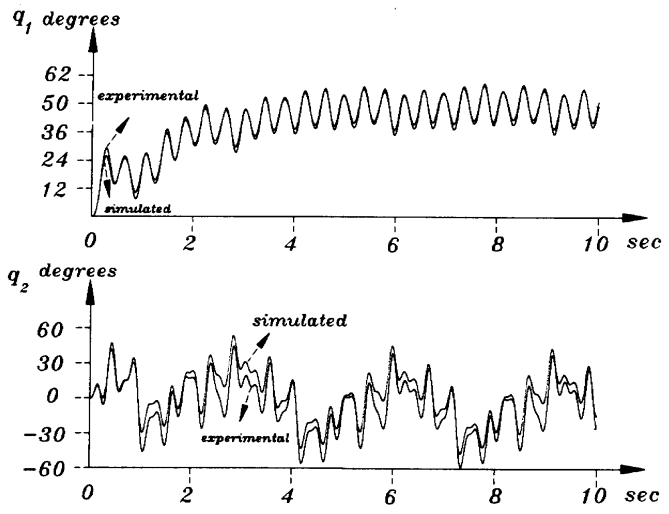


Fig. 4. Simulated and experimental responses; case filtered dynamic model.

simulation with these estimated parameters follow the shape of the experimental responses obtained on the actual robot.

6.2 Supplied energy model

Figure 5 depicts the evolution in time of the vector of estimated parameters by using the supplied energy regression model. The value of the estimated parameter are listed in Table II. For this identification scheme we remark that five of the nine parameters do not converge adequately, rather diverging and furthermore they are found in small oscillations. This is the case of the components $\hat{\theta}_5(k) - \hat{\theta}_9(k)$. This phenomenon can be attributed to the following: The supplied energy approach employs integrators in some components of the regressor; they have infinite-gain at zero frequency and they amplify low frequency noise. This is particularly true for the entries of the regressor corresponding to Coulomb coefficients. Hence, these components of the regressor keep large values owing to the low-frequency of sgn $(\dot{\boldsymbol{q}})$ leading offsets and drifts.[11] This drawback of the supplied energy regression model is overcome with the filtered power regression model which instead of integrators involves low-pass filters with unit gain at zero frequency.

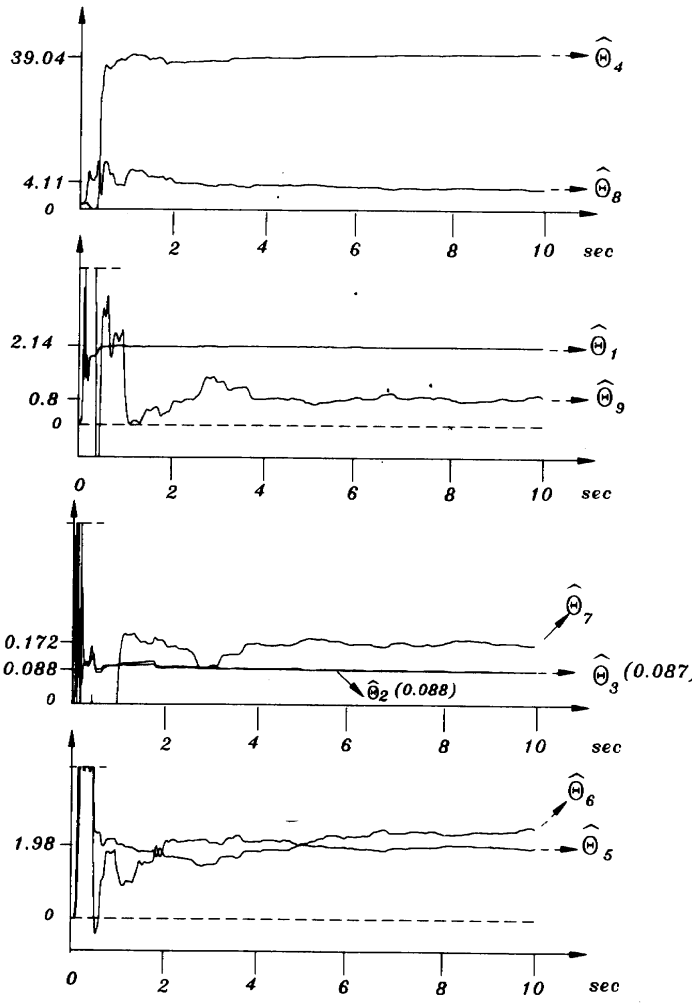


Fig. 5. Estimated vector $\hat{\boldsymbol{\theta}}$ of the supplied energy model.

https://doi.org/10.1017/S0263574797000659 Published online by Cambridge University Press

Table II.

	Measured	Supplied Energy	Filtered Power	Filtered Dynamic	Unit
θ_1	2.351	2.14	1.99	1.98	Nm-sec^2
θ_2	0.084	0.088	0.084	0.087	Nm
θ_3	0.102	0.087	0.084	0.084	Nm-sec^2
θ_4	38.465	39.04	36.20	38.48	Nm
θ_5	1.825	—	2.01	1.99	Nm
θ_6	2.288	—	2.35	2.11	Nm-sec
θ_7	0.175	—	0.192	0.120	Nm-sec
θ_8	7.60	—	4.95	6.20	Nm
θ_9	1.734	—	1.01	1.18	Nm

Because the lack of convergence of some of the estimated parameters, we have not performed any open-loop simulation with the estimated parameters.

6.3 Filtered power model

Figure 6 shows the vector of estimated parameter $\hat{\boldsymbol{\theta}}(k)$ plotted versus time using the filtered power regression model. In contrast with the supplied energy model, in this identification scheme the oscillations in the components $\hat{\theta}_5(k) - \hat{\theta}_9(k)$ of the estimated vector are reduced significantly and in spite of excessive excursions of some estimated parameters after the initial transient, we can observe that there exists parameter convergence for all the components of parameter vector. The value of estimated parameters are summary in the Table II. The deviation of these parameters (excluding the friction parameters) with respect to the nominal ones obtained via direct measurement is in between 82–94%. However the estimated Coulomb coefficients have a larger deviation.

Figure 7 shows a comparison between the real joint positions and the simulated joint positions with the identified parameters obtained with the identification scheme using the filtered power regression model. In this case the results show good features, however it does not improve the results obtained with the filtered dynamic model. This may be attributed to the fact that the latter involves a vector prediction error being more rich in information.[4]

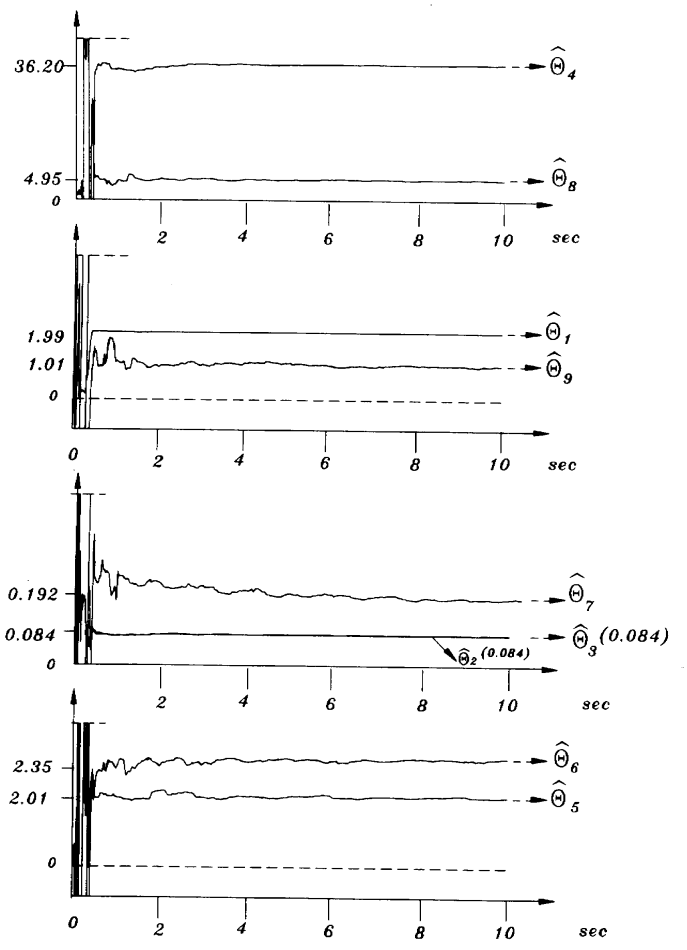


Fig. 6. Estimated vector $\hat{\boldsymbol{\theta}}$ of the filtered power model.

6.4 Discussion

The experimental results allow the conclusion that the identification schemes based on the filtered dynamic and filtered power models are clearly superior to the one based on the supplied energy model. Notwithstanding, in case of knowledge of the Coulomb coefficients and their use for friction compensation, the supplied energy model should have similar performances that the filtered power model.

The identification scheme based on the filtered dynamic regressor model has a vector prediction error.

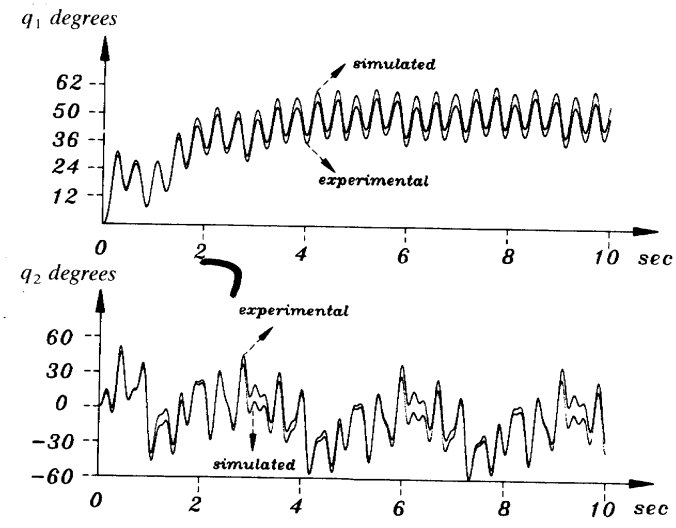


Fig. 7. Simulated and experimental responses; case filtered power model.

https://doi.org/10.1017/S0263574797000659 Published online by Cambridge University Press

Therefore it is more complex to implement and it consumes more calculation time, while the identification schemes based on the supplied energy and filtered power regressor models is made up with one scalar prediction error which saves a lot of computational effort by avoiding the need of calculating more data.

The experimental results indicate deviations of the estimated parameters with respect to the nominal ones. Possible explanations are the following.

- The joint velocity $\dot{\boldsymbol{q}}$ used in the regressors has not been directly measured by any sensor but it has been computed via numerical differentiation of joint position $\boldsymbol{q}$. This fact introduces an approximation for the velocity value which causes deviation of the estimated parameters.
- In our experimental robot, the Coulomb coefficient for the first joint is not constant. It takes two different values of depending from the sense of motion. Therefore the corresponding component of the vector of estimated parameters do not converge to none of its real values. This also will have influence on the convergence of the other components. This is may be the main reason why the estimated Coulomb coefficients obtained from all the identification schemes differ notably from the nominal values.

7 CONCLUSION

In this paper we have presented the experimental evaluation of three identification schemes to determine the dynamic parameters for a two degrees of freedom direct-drive robot.

The identification schemes are composed by an underling standard recursive least-squares algorithm with three regression models. The considered schemes are based on the following regression models: filtered dynamic, supplied energy and filtered power models.

The filtered dynamic model scheme presents the best results in the estimated parameters, however, it is the more complex to implement. On the other hand, the supplied energy and filtered power models reduce the computational burden and therefore they are more suitable for real-time implementation.

In case of absence of friction or friction compensation, the supplied energy and filtered power models may perform in a similar way; however, if Coulomb friction is present, the filtered power model offers advantage over the approach based on the supplied energy model.

Besides the exact knowledge of the structure of the robot dynamics and the suitable choice of the torque input signal, for good robot identification we believe that accurate joint velocity information plays an important role on the final results.

ACKNOWLEDGMENTS

The authors would like to thank Marc Feyh from Parker Compumotor for providing us with useful information on

REFERENCES

1. P. Khosla and T. Kanade, "Parameter identification of robot dynamics" *Proceedings of 24th Conference on Decision and Control,* Ft. Lauderdale Fl, (1985) pp. 1754–1760.
2. C.G. Atkeson, C.H. An and J.M. Hollerbach, "Estimation of inertial parameters of manipulator loads and links" *Int. J. Robotics Research* **5,** No. 3, 101–118, (1986).
3. M. Prüfer, C. Schmidt and F. Wahl, "Identification of robot dynamics with differential and integral models: a comparison" *Proceedings IEEE International Conference on Robotics and Automation,* San Diego, California (1994) **Vol. 1,** pp. 340–345.
4. K.R. Kozlowski and P. Dutkiewicz, "Experimental identification of robot and load dynamics" *13th IFAC World Congress,* San Francisco, USA, (1996) Preprints Vol. A, pp. 397–402.
5. P.R. Shirkey, "A testbed for intelligent control" *Thesis of Master of Science* (University of Illinois at Urbana-Champaign, 1996).
6. P. Hsu, M. Bodson, S. Sastry and B. Paden, "Adaptive identification and control for manipulators without using joint accelerations" *Proceedings of IEEE International Conference on Robotics and Automation,* Raleigh, C.N., (1987) pp. 1210–1215.
7. B. Armstrong, O. Khatib and J. Burdick, "The explicit dynamic model and inertial parameters of the PUMA 560 arm" *Proceedings of the IEEE International Conference on Robotics and Automation,* (1986). pp. 510–518.
8. C. Canudas and A. Aubin, "Parameters identification of robot manipulators via sequential hybrid estimation algorithms" *Proc. IFAC'90 Congress,* Tallin, (1990) pp. 178–183.
9. W. Khalil and P.P. Restrepo, "An efficient algorithm for the calculation of the filtered dynamic model of robots" *Proc. of IEEE International Conf. on Robotics and Automation,* Minneapolis, MN (1996) pp. 323–328.
10. J.J.E. Slotine and W. Li, "Adaptive robot control: a new perspective" *Proceedings of the 26th Conference on Decision and Control,* Los Angeles, CA, (1987) pp. 192–198.
11. Z. Lu, K.B. Shimoga and A.A. Goldenberg, "Experimental determination of dynamic parameters of robotic arms" *J. Robotic Systems* **10**(8), 1009–1029 (1993).
12. M. Gautier and W. Khalil, "On the identification of the inertial parameters of robot" *Proceedings of the 27th Conference on Decision and Control,* Austin, Texas (1988) pp. 2264–2269.
13. C. Canudas, P. Noel, A. Aubin and B. Brogliato, "Adaptive friction compensation in robot manipulators: low velocities" *Int. J. Robotics Research* **10,** No. 3, 189–199 (1991).
14. M.W. Spong and M. Vidyasagar, *Robot Dynamics and Control* (John Wiley and Sons, NY., 1989).
15. K.J. Åström and B. Wittenmark, *Adaptive Control* (Addison-Wesley, Reading, MA, 1989).
16. G.C. Goodwin and K.S. Sin, *Adaptive Filtering Prediction and Control* (Prentice-Hall, NY, 1984).
17. C.H. An, C.G. Atkeson and J.M. Hollerbach, *Model Based Control of a Robot Manipulator* (The MIT Press, Cambridge, Mass., 1989).
18. F. Reyes and R. Kelly, "A direct-drive robot for control research" *Proceedings of the IASTED International Conference, Applications of Control and Robotics,* Orlando, Fl. USA (1996) pp. 181–184.
19. Yokogawa, *Direct drive servo actuator-general specification* (*GS A101-E*) (Yokogawa Electric Corp., Tokyo, Japan, 1988).
20. B. Armstrong, "On finding exciting trajectories for identification experiments involving systems with nonlinear dynamics" *Proc. of IEEE International Conf. on Robotics*

https://doi.org/10.1017/S0263574797000659 Published online by Cambridge University Press